SUPPORTING INFORMATION

Inhibition of alpha-synuclein fibril elongation by Hsp70 is governed by a kinetic binding competition between alpha-synuclein species

Francesco A. Aprile, Paolo Arosio, Giuliana Fusco, Serene W. Chen, Janet R. Kumita, Anne Dhulesia, Paolo Tortora, Tuomas P. J. Knowles, Michele Vendruscolo, Christopher M. Dobson & Nunilo Cremades

Supplementary Materials and Methods

Protein expression and purification. Recombinant N-hexa-His-tagged Hsp70 (Hsp70 1A, gi:194248072) was expressed and purified from *E.coli* BL21 (DE) gold strain (Stratagene, San Diego, CA, USA) as previously described [1, 2]. Thrombin cleavage efficiency and protein purity exceeded 95% as determined by mass spectrometry and SDS–PAGE analysis. Protein concentration was determined by absorbance measurements at 280 nm, using theoretical extinction coefficients calculated with Expasy ProtParam [3]. Human wild-type (gi:80475099) and mutant A90C αSyn variants were purified as previously reported [4]. Protein purity exceeded 98% as determined by mass spectrometry and SDS–PAGE analysis, and concentrations were determined by absorbance measurements at 275 nm using an extinction coefficient of 5600 M^{-1} cm^{-1}.

Labeling reaction. The A90C αSyn variant was labeled either with DANSYL-MTS (Toronto Research, Toronto, Canada) or Alexa Fluor 488 C5 maleimide (Thermo Fisher Scientific, Waltham, MA, USA) via the cysteine thiol moiety. The protein was incubated in the dark (3h at room temperature or over night at 4°C) in the presence of a 5 molar equivalent excess of the dye in in 50 mM Tris pH 7.4, 150 mM KCl, 5 mM $MgCl_2$. The labeled proteins were then purified from the remaining free dye using a P10 desalting column containing a Sephadex G25 matrix (GE

Healthcare, Little Chalfont, UK). The samples with the labeled proteins were divided into aliquots, flash frozen and stored at -80 °C. Each aliquot was thawed immediately prior to use. The labeling efficiency was greater than 90% as estimated by mass spectrometry. The labeled protein concentration was determined by absorbance measurements at 335 and 495 nm using the extinction coefficient of the free dye 4100 or 73000 M^{-1} cm^{-1}, for dansylated and A488 conjugated proteins, respectively [4,(5)].

Fluorescence titration with monomeric dansylated αSyn. The procedure was based on previous studies of the characterization of Hsp70 binding to a wide range of substrates [(1, 2, 6, 7)]. Fluorescence titration experiments were carried out by incubating dansylated αSyn (2 μM in 50 mM Tris pH 7.4, 150 mM KCl, 5 mM $MgCl_2$) for 30 min at 25°C in the presence of different chaperone concentrations in the presence or absence of 5 mM ATP. Fluorescence emission spectra from 400 to 630 nm were recorded as the average of 10 scans, following excitation at 330 nm [(1)]; the increase in fluorescence intensity at the emission maximum was plotted as a function of Hsp70 concentration, and analyzed assuming a single binding site model using the following equation:

$$F = \frac{F_{max}\,[chaperone]}{K_d + [chaperone]}$$

where F is the fluorescence intensity observed at a given concentration of free Hsp70 in equilibrium (for practical reasons this was approximated to be the total Hsp70 concentration), F_{max} is the fluorescence intensity at saturation and K_d is the apparent dissociation constant of the complex.

Aggregation conditions. αSyn alone (70 μM) or with Hsp70 (7 μM; i.e. 1:10 chaperone-to-αSyn molar ratio) was incubated in 600 μl of 50 mM Tris pH 7.4, 150 mM KCl, 5 mM $MgCl_2$ (with 0.01% NaN_3 to prevent bacterial growth) at 37°C under constant shaking at 200 rpm. Where specified, samples contained 2 mM ATP and an ATP-buffer system (0.2 units/ml pyruvate kinase and 5 mM phosphoenol pyruvate). At specific incubation times, 10 μl aliquots were analyzed for the quantity of soluble protein amount or for Thioflavin T (ThT) binding. For ThT analysis, samples were incubated with ThT (20 μM) for 30 min. Fluorescence emission was recorded as the

average of three spectra from 460 to 600 nm, following excitation at 446 nm using a Cary Eclipse fluorescence spectrophotometer (Varian Inc., Palo Alto, CA, USA). ThT results are reported as relative fluorescence intensity; densitometry data are represented as insoluble protein fractions, normalizing them to the values corresponding to the concentration of initial soluble protein and plotting the reciprocal values.

Seeded aggregation experiments. Monomeric αSyn alone (70 μM) or with increasing concentrations of Hsp70 was incubated in the presence of 5% preformed second generation fibrils in 50 mM Tris pH 7.4, 150 mM KCl, 5 mM $MgCl_2$, 0.01% NaN_3, 20 μM ThT at 37°C without shaking. The reaction was performed in the presence of 5 mM ATP, and ThT fluorescence was monitored in low-binding, clear-bottomed half-area 96-well plates (Corning Inc., New York, NY, USA). Emissions at 480 nm was recorded every 5 min with excitation at 440 nm, using a CLARIOstar plate reader (BMG Labtech, Ortenberg, Germany). Second generation fibrils were prepared as follows: monomeric αSyn (70 μM, 300 μl) was incubated in 50 mM Tris pH 7.4, 150 mM KCl, 5 mM $MgCl_2$ (with 0.01% NaN_3 to prevent bacterial growth) at 37°C under constant shaking at 200 rpm for 4 days. The fibrillar pellets were centrifuged (16000 X g, 30 min) and washed twice with buffer (300 μl). Fibrils were resuspended at a concentration of 100 μM and sonicated (1 min, 10% max power, 30% cycles) using a probe sonicator (Bandelin, Sonopuls HD 2070, Bandelin Elec., Germany) in order to produce first generation seeds. Second generation fibrils were prepared by incubating monomeric αSyn (100 μM) in the presence of first generation seeds (10 μM) in 50 mM Tris pH 7.4, 150 mM KCl, 5 mM $MgCl_2$, 0.01% NaN_3 (500 μl) at 37°C under quiescent conditions for 13-14 h. The suspension was finally sonicated (20 s, 10% max power, 30% cycles).

Immunogold-labeling transmission electron microscopy (TEM). Hsp70 (10 μM) was incubated in the presence of 1 monomer equivalent of second-generation seeds (30 min, RT). The suspension was centrifuged (15 min, 16000 X g) and the fibrillar pellets were washed with buffer. 5 μl aliquots of sample were applied to a carbon support film, 400 mesh, 3 mm nickel grid (TAAB Laboratories Equipment Ltd, Berks, UK) and incubated (5 min, RT). The grid was blocked with 1 mg/mL BSA

(NEB, Ipswich, MA, USA) in PBS for 15 min and incubated with 1:100 monoclonal antibody against human Hsp70 (C92F3A-5, Abcam, Cambridge, UK) in PBS for 30 min. The grid was washed (3 x 5 min); first in PBS/0.01% Triton/0.01% Tween-20 and then twice with PBS only, followed by incubation with 1:500 secondary gold antibody in PBS for 30 min. Finally the grid was washed three times as described above, twice with water and then incubated for 2 min with 2% uranyl acetate (w/v). In order to remove excess uranyl acetate, the grid was washed twice with water and dried completely before imaging. The fibrils with bound Hsp70 were imaged on a FEI Tecnai G_2 transmission electron microscope (Multi-Imaging Unit in the Department of Physiology, Development and Neuroscience, University of Cambridge, UK). Images were analyzed using the SIS Megaview II Image Capture system (Olympus, Tokyo, Japan).

Atomic Force Microscopy (AFM). AFM images were taken with a Nanowizard II atomic force microscope (JPK, Berlin, Germany) using tapping mode in air. Fibril suspensions were diluted to below 1 μM in water and 10 μl aliquots were deposited on freshly cleaved mica and left to dry. The lengths and heights of the fibrils were manually derived from a sample of 1000 fibrils (Figure S1). The number of monomers per seed fibril (which was used for the estimation of the growth rate in the kinetic analysis of the seeded aggregation experiments and of the binding affinity for the fibrils) was calculated using the following equation:

$$N = \frac{\rho\, V\, N_A}{MW} = \frac{\rho\, \pi\, \left(h/2\right)^2 l\, N_A}{MW}$$

where N is the number of monomers per seed, N_A is the Avogadro's constant, MW the molecular weight, p is density (=1.35g/cm^3), V the volume, h and l the height and the length, respectively, of the fibrils (derived from AFM). The number of monomers per seed fibril was estimated by this means to be 60 ± 10.

Kinetic analysis. Under seeded conditions, the time evolution of the total fibril mass concentration, *M(t)*, is governed mainly by elongation events according to the equation:

$$\frac{dM}{dt} = 2k_+Pm$$
$$m(t) = M_0 - M(t)$$

Where *P* is the number of fibrils (equal to the initial concentration of seed fibrils, P_0, estimated by AFM, see previous section) and *m* is the concentration of soluble monomeric αSyn.

Hsp70 can interfere with the elongation process by interacting either with fibril ends or with soluble monomers. We can discriminate between these two situations by considering explicitly the binding reactions in the kinetic model, and by comparing the corresponding model simulations with the experimental data. The K_d of binding for Hsp70 to monomeric αSyn ($K_{d,M}$) was taken to be 1.8 μ M, which is the value of the K_d estimated by fluorescence titration experiments in the presence of ATP (Figure 1 in the main text). The K_d of binding of Hsp70 to αSyn fibril ends ($K_{d,F}$) was considered unknown. The $K_{d,F}$ reported is the one which corresponds to the best fit. In order to avoid a significant contribution of the binding of the chaperone to the surface of the fibrils, which would have complicated the analysis of the elongation reaction, we have confined our analysis to the first two hours of aggregation.

Total monomer consumption at the end of the elongation reactions was proved by intrinsic protein fluorescence measurements on the soluble fraction (Figure S8). The fluorescence intensity values at the end of the reactions were then taken as formation of 100% fibrils in order to determine the fraction of fibrils formed at any time of the reaction. The elongation kinetic data was then plotted as "Fraction of fibrils formed" that refers to the mass concentration of fibrils generated by fresh monomers, excluding the initial concentration of seeds.

a) Kinetic model involving interactions with fibril ends

We distinguish three classes of fibrils: fibrils with no ends occupied by Hsp70, fibrils with only one end blocked by the chaperone, and fibrils where Hsp70 is bound to both ends. The number concentration of the three classes is defined as *P*, *P'* and *P''*,

respectively. The corresponding mass balance equations governing the time evolution of these quantities, together with the total fibril mass (M), the free monomer in solution (m) and the concentration of the free chaperone in solution (C^{Hsp70}_{free}) are:

$$\frac{dm}{dt} = -2k_+Pm - k_+P'm$$
$$\frac{dM}{dt} = 2k_+Pm + k_+P'm$$
$$\frac{dP}{dt} = -2k_{on,F}PC^{Hsp70}_{free} + k_{off,F}P'$$
$$\frac{dP'}{dt} = 2k_{on,F}PC^{Hsp70}_{free} - k_{off,F}P' - k_{on,F}P'C^{Hsp70}_{free} + k_{off,F}P''$$
$$\frac{dP''}{dt} = k_{on,F}P'C^{Hsp70}_{free} - k_{off,F}P''$$
$$\frac{dC^{Hsp70}_{free}}{dt} = -2k_{on,F}PC^{Hsp70}_{free} + k_{off,F}P' - k_{on,F}P'C^{Hsp70}_{free} + k_{off,F}P''$$

Where k_+ is the elongation rate constant, and $k_{on,F}$ and $k_{off,F}$ are the association and dissociation rate constants for the chaperone to the fibril end, respectively. All concentrations are in moles.

$P + P' + P'' = P_0$ (Initial number of seeds)
$C^{Hsp70}_{free} + P' + 2P'' = C_0$ (Initial concentration of Hsp70)

b) Kinetic model involving interactions with monomers

$$\frac{dm}{dt} = -2k_+P_0m - k_{on,M}C^{Hsp70}_{free}m + k_{off,M}C^{Hsp70}_{bound}$$
$$\frac{dC^{Hsp70}_{bound}}{dt} = 2k_{on,M}C^{Hsp70}_{free}m - k_{off,M}C^{Hsp70}_{bound}$$
$$C^{Hsp70}_{bound}(t) = C^{Hsp70}_0 - C^{Hsp70}_{free}$$

Where $k_{on,M}$ and $k_{off,M}$ are the association and dissociation rate constants for the chaperone to the fibril end, respectively.

c) Kinetic model involving interactions with both fibril ends and monomers

The kinetic model involving interactions with both fibril ends and monomers represents the simple combination of the two previous models.

The model simulations were globally fitted to the experimental data through a least squares procedure by minimizing an error function defined as: where $y(t)_{sim}$ is the simulated mass fraction and $y(t)_{exp}$ is the experimentally measured mass fraction at a given incubation time t and at a molecular chaperone concentration *Ci*.

$$Y(error) = \sum_{i=1}^{N} \sum_{j=1}^{t_{MAX}} \left(Y_{i,j}^{SIM} - Y_{i,j}^{Exp}\right)$$

N = number of concentrations of Hsp70

t_{MAX} = number of time point per concentration

Fluorescence polarization (FP) measurements. Solutions of 0.5 µM Alexa488-αSyn were incubated in the presence of increasing concentrations of Hsp70 (between 0.5 and 20 µM) in 50 mM Tris pH 7.4, 150 mM KCl, 5 mM $MgCl_2$, 5 mM ATP at room temperature. FP was monitored in black-bottom costar 96 well plates (Corning Inc., New York, NY, USA) at 520 nm every 60 seconds (excitation at 480 nm), using a CLARIOstar plate reader (BMG Labtech, Ortenberg, Germany). We observed a systematic and reproducible decrease of FP of Alexa488-αSyn when the sample was diluted with buffer (Figure S6a, 0 µM Hsp70). This decrease was observed even when the sample was initially left to reach steady-state conditions and a smaller sample dilution was then applied (Figure S6b, 0 µM Hsp70). Therefore, the behavior of FP of Alexa488-αSyn upon sample dilution under our experimental conditions was also taken into account when globally analyzing the kinetic data of association of the chaperone to monomeric αSyn for a given experimental set of data. These changes in FP upon sample dilution was successfully simulated in all cases as a monoexponential function (see experimental and fit data for 0 µM Hsp70 in Figure S6a,b), whose parameters were constant for a given experimental set of data (i.e. for all the chaperone concentrations tested at otherwise identical conditions).

The FP experiments were performed under pseudo-first order conditions. Under these conditions, the free chaperone concentration can be assumed to be equal to the total chaperone concentration at all chaperone concentrations used, and the variations of the FP signal with time then follow a monoexponential function [8], as it

can be evidenced after subtracting the changes in FP due to sample dilution (see Figure S6c). The different kinetic traces at different chaperone concentrations obtained for a given set of experimental data was then globally analyzed (using Origin 7.0) and the observed kinetic constants for the association process at each chaperone concentration was then plotted as a function of chaperone concentration. As expected, a good linear correlation was obtained (Figure S6d); the slope of the linear regression line corresponds to the estimate of the second-order rate constant for association of the chaperone to monomeric αSyn, $k_{on,M}$ [9].

Intrinsic Protein Fluorescence Measurements. Samples from aggregation mixtures of 70 μM monomeric αSyn in the presence of 0.5% seeds were collected at the beginning and at the end of the aggregation reaction and ultracentrifuged for 30 min at 90,000 rpm (using a TLA-100 Beckman rotor). Intrinsic fluorescence emission spectra of the supernatants were recorded as the average of three spectra from 280 to 400 nm, following excitation at 275 nm using a Cary Eclipse fluorescence spectrophotometer (Varian Inc., Palo Alto, CA, USA).

Table S1. Kinetic and thermodynamic constants derived from the global fit.

	k_+ (1/M/s)	$k_{on,M}$ (1/M/s)	$K_{d,M}$ (µM)	$k_{on,F}$ (1/M/s)	$K_{d,F}$ (µM)
Model a	500	100	1.8	-	-
Model b (kinetic competition)	500	1	1.8	230	9
Model c (thermodynamic competition	500	230	1.8	230	0.18

Supplementary Figures

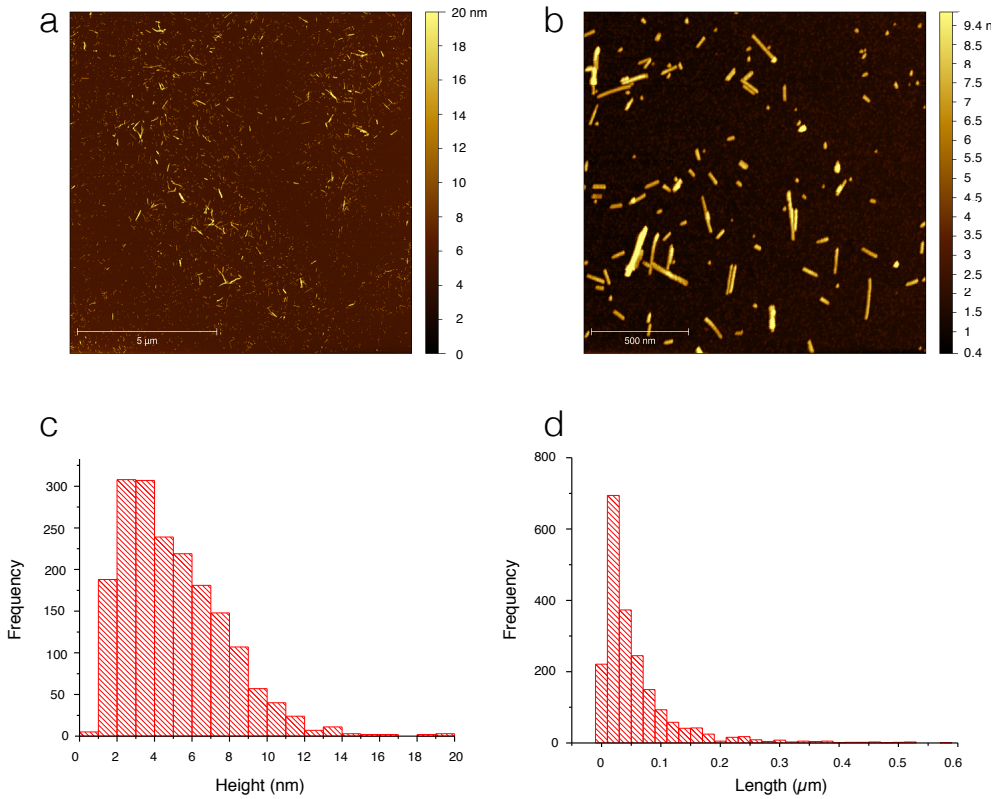

Figure S1. (a,b) AFM analysis of the αSyn seeds used in the seeding experiments. Distribution of the heights (c) and lengths (d) of the seeds.

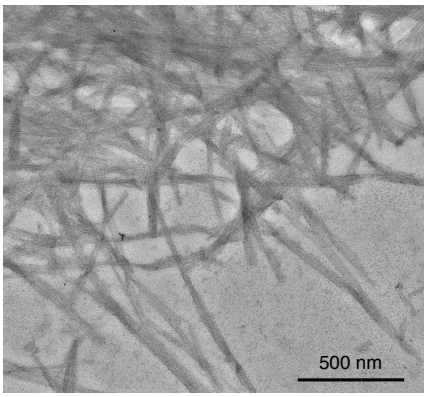

Figure S2. Control Immuno-TEM images of αSyn fibrils in the absence of FL-Hsp70. The samples were treated with the Hsp70 primary and gold-labeled secondary antibodies, as for the images shown in Figure 1c in the main text. The scale bar represents 500 nm.

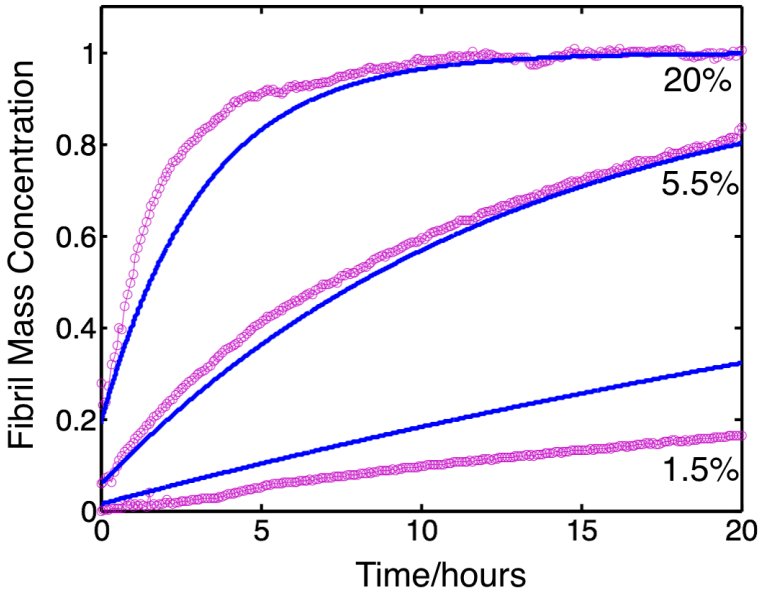

Figure S3. Estimation of the fibril elongation rate constant by fitting the results of the ThT reaction profiles of αSyn in the presence of 1.5, 5.5 and 20 % preformed seeds (showed in Figure S1) without chaperone.

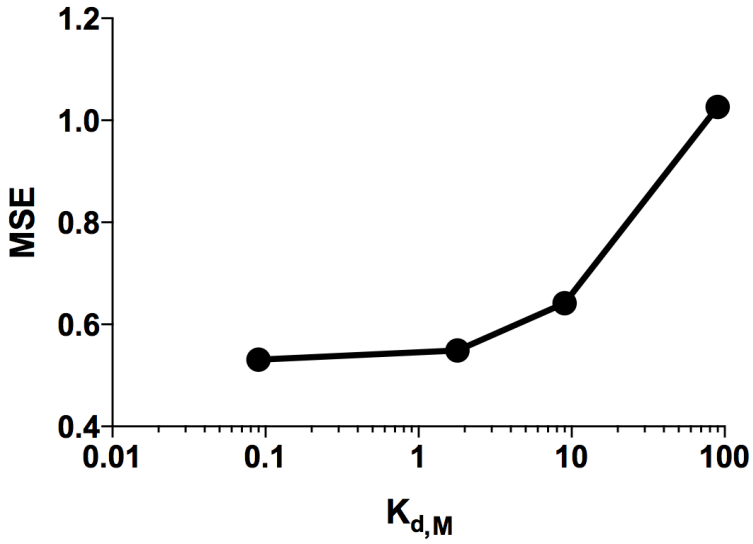

Figure S4. Variation of the mean squared error for the best fit of the kinetic experimental data to a model considering the binding of Hsp70 to monomeric αSyn only and assuming different values of $K_{d,M}$.

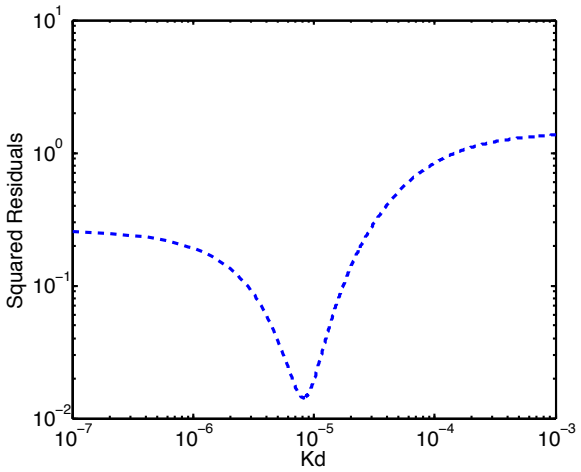

Figure S5. Squared residuals of the best fits of the experimental kinetic data for αSyn fibril elongation in the presence of Hsp70 to a global analysis assuming a model where the chaperone can bind only to both αSyn monomers and fibril ends as a function of the $K_{d,F}$ value.

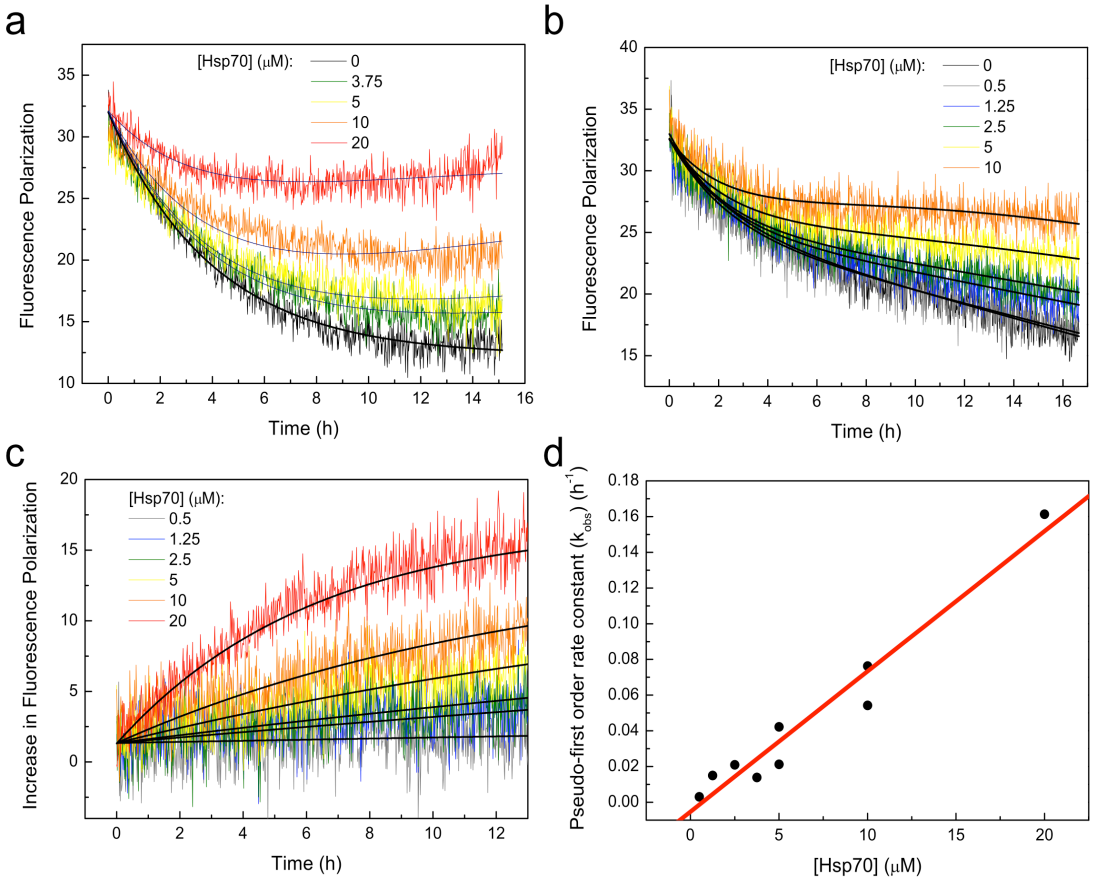

Figure S6. Kinetic traces for chaperone:αSyn complex formation followed by fluorescence polarization. (a,b) FP kinetics of monomeric A488-αSyn upon addition of solutions of different concentrations of Hsp70. Black lines correspond to the best fit of the data to a double monoexponential function where the parameters of the monoexponential function that simulate the FP changes associated to sample dilution are shared to all the kinetic traces for a given experimental set. (a) and (b) are examples of experiments where different sample dilution and pre-equilibration times were used. (c) Experimental and best fit kinetic traces to a monoexponential function at different chaperone concentrations after subtracting the contribution of sample dilution. (d) Plot representing the pseudo-first order rate constants obtained experimentally for each chaperone concentration analyzed as a function of chaperone concentration (black points). The best fit to a linear correlation for all the experimentally obtained pseudo-first order rate constants is represented as a red line; the slope of this line represents a good estimate for the second-order rate constant for association of the chaperone to monomeric αSyn, $k_{on,M}$.

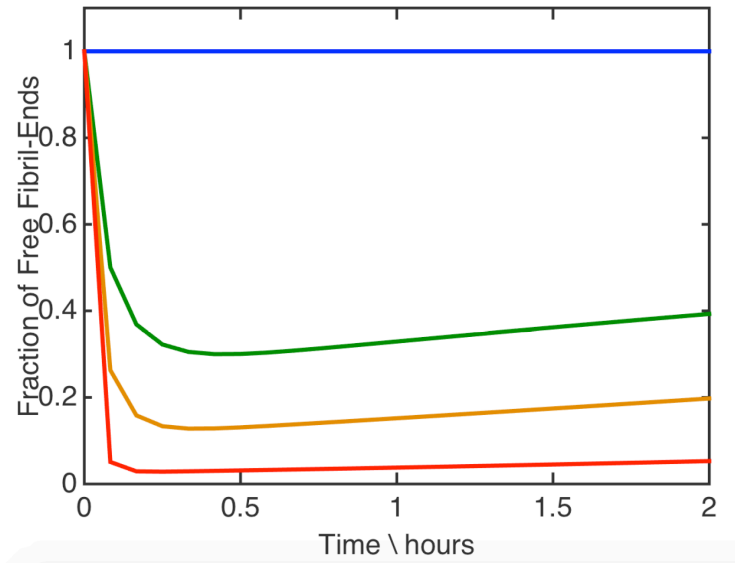

Figure S7. Fraction of fibril ends free to elongate as a function of time during kinetic elongation experiments in the presence of the different chaperone concentrations (from blue to red; 0, 7, 14, 35 µM). The fraction of free fibril ends was calculated for each kinetic condition according to the best fit of the experimental data to a model where the chaperone can bind to both monomeric and fibrillar αSyn through a binding kinetic competition (fits presented in Figure 2b, centre panel, in the main text).

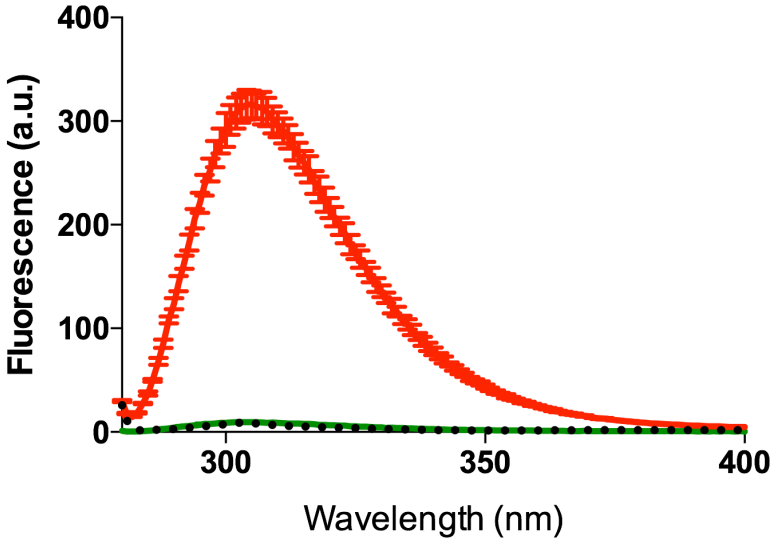

Figure S8. Quantification of monomeric αSyn left in solution at the end of the aggregation reaction. Intrinsic protein fluorescence emission spectra of the soluble fraction of samples collected at the beginning (red line) or at the end (green line) of the aggregation reaction of 70 µM monomeric αSyn in the presence of 5% seeds. The spectrum of the buffer is shown as a black dashed line. Each spectrum is the average of three individual replica and the error bars represent the standard deviation.

Supplementary References

1. Roodveldt, C., Bertoncini, C. W., Andersson, A., van der Goot, A. T., Hsu, S. T., Fernández-Montesinos, R., de Jong, J., van Ham, T. J., Nollen, E. A., Pozo, D., Christodoulou, J., and Dobson, C. M. (2009) Chaperone proteostasis in Parkinson's disease: stabilization of the Hsp70/alpha-synuclein complex by Hip., *EMBO J 28*, 3758-3770.
2. Aprile, F. A., Dhulesia, A., Stengel, F., Roodveldt, C., Benesch, J. L., Tortora, P., Robinson, C. V., Salvatella, X., Dobson, C. M., and Cremades, N. (2013) Hsp70 oligomerization is mediated by an interaction between the interdomain linker and the substrate-binding domain, *PLoS One 8*, e67961.
3. Gill, S. C., and von Hippel, P. H. (1989) Calculation of protein extinction coefficients from amino acid sequence data., *Anal Biochem 182*, 319-326.
4. Cremades, N., Cohen, S. I., Deas, E., Abramov, A. Y., Chen, A. Y., Orte, A., Sandal, M., Clarke, R. W., Dunne, P., Aprile, F. A., Bertoncini, C. W., Wood, N. W., Knowles, T. P., Dobson, C. M., and Klenerman, D. (2012) Direct Observation of the Interconversion of Normal and Toxic Forms of α-Synuclein., *Cell 149*, 1048-1059.
5. Gasymov, O. K., Abduragimov, A. R., and Glasgow, B. J. (2010) Excited protein states of human tear lipocalin for low- and high-affinity ligand binding revealed by functional AB loop motion., *Biophys Chem 149*, 47-57.
6. Schlecht, R., Erbse, A. H., Bukau, B., and Mayer, M. P. (2011) Mechanics of Hsp70 chaperones enables differential interaction with client proteins., *Nat Struct Mol Biol 18*, 345-351.
7. Buczynski, G., Slepenkov, S. V., Sehorn, M. G., and Witt, S. N. (2001) Characterization of a lidless form of the molecular chaperone DnaK: deletion of the lid increases peptide on- and off-rate constants., *J Biol Chem 276*, 27231-27236.
8. Ahmad, S., Pecqueur, L., Dreier, B., Hamdane, D., Aumont-Nicaise, M., Plückthun, A., Knossow, M., and Gigant, B. (2016) Destabilizing an interacting motif strengthens the association of a designed ankyrin repeat protein with tubulin, *Sci Rep 6*, 28922.
9. Rutkowska, A., Mayer, M. P., Hoffmann, A., Merz, F., Zachmann-Brand, B., Schaffitzel, C., Ban, N., Deuerling, E., and Bukau, B. (2008) Dynamics of trigger factor interaction with translating ribosomes, *J Biol Chem 283*, 4124-4132.